Nonlinear Dyn (2008) 52: 377–393
DOI 10.1007/s11071-007-9286-2

ORIGINAL PAPER

# Application of joint coordinates and homogeneous transformations to modeling of vehicle dynamics

**Marek Szczotka · Stanisław Wojciech**

Received: 12 February 2007 / Accepted: 30 May 2007 / Published online: 25 July 2007


**Abstract** The paper presents a method of modeling dynamics of multibody systems with open and closed kinematic chains. The joint coordinates and homogeneous transformations are applied in order to formulate the equations of motion of a rigid body. In this method, constraint equations are introduced only in the case when closed subchains are considered or when the joint reactions have to be calculated. This allows the number of generalized coordinates in the system to be reduced in comparison to the case when absolute coordinates are applied. It is shown how the method can be applied to modeling of vehicle dynamics. The calculation results are compared with those obtained when the ADAMS/Car package is used. Experimental verification has been performed and is reported in the paper, as well. In both cases, a good correspondence of results has been achieved. Final remarks concerning advantages and disadvantages of the method are formulated at the end of the paper.

**Keywords** Homogeneous transformations · Joint co-ordinates · Multibody and vehicle dynamics

M. Szczotka (✉)
University of Bielsko-Biała, ul. Willowa 2, 43-309 Bielsko-Biała, Poland
e-mail: marek.szczotka@axtech.no

S. Wojciech
Automotive Research and Development Centre BOSMAL, ul. Sarni Stok 1, 43-300 Bielsko-Biała, Poland

## 1 Introduction

Multibody dynamics is a discipline of mechanics which has a wide range of applications. Research and development in many branches of industry, such as machines and mechanisms, ground vehicles, aircraft or biomechanics are based on the use of mathematical models and simulation tools. A large number of books and papers have been published in this field. Some of them concern only rigid systems [1] while others deal with mixed rigid-flexible [2, 3] multibody systems. An overview can be found in [4].

The most frequent formalism in description of location and orientation of bodies in three dimensional space is based on absolute coordinates. Application of the Lagrange equations leads to a set of differential-algebraic equations (DAE). The second order, ordinary differential equations of motion are completed by a set of nonlinear constraint equations [2]. The DAE for mechanical systems are characterized by index 3, which is reported by many researchers as a source of problems during numerical integration. Many studies have been carried out in order to improve the stability and effectiveness of the numerical methods applied. The work in this area was initiated by Gear [5] and Petzold [6]. One of the first and well-known methods that allows the numerical solution of constrained multibody systems to be achieved, is the Baumgarte stabilization method [7]. More information about algorithms for integrating DAE and application to vehicle dynamics is presented in [8].

The absolute coordinates are used so frequently because they allow an automatic generation of equations of motion and constraint equations. Many software packages have been developed, and they are widely used as general purpose multibody simulation codes, [9–12]. Frequently, multibody models of rigid systems are coupled with flexible structures, and the resulting systems of bodies are analyzed together [13]. This is an effective approach, which enables a wide-ranging study of vibrational problems of mechanical structures.

In the last few years, multibody dynamics has become part of an interdisciplinary research area focused on comprehensive research of virtual prototyping. The mechanical structures of newly developed vehicles, machines, trains, etc. are full of electronics and control subsystems. Good examples are vehicles with active and semi-active suspensions [14–16]. This approach allows us to study control strategies and a controller's influence on dynamic performance of almost every multibody structure [17].

General multibody models and algorithms are an example of complex computer codes. On the other hand, in some applications (real-time calculations, controls, virtual reality, etc.), it is necessary to achieve fast simulations, even much faster than real time. Interesting examples from this field can be found in [3]. The method of analysis of open and closed chains of multibody systems based on equivalent systems of particles is shown in paper [18]. In this approach, an elimination of internal reaction forces is carried out and the minimal set of equations is achieved. This method is an attempt to reduce disadvantages caused by the large number of constraints generated in algorithms based on description in absolute coordinates and by the full geometric complexity of the system.

Application of relative joint coordinates to a description of system dynamics, is fairly rare. This method results in a system of ordinary differential equations (ODE) without constraint equations when open loops are analyzed. This method also leads to a minimal number of generalized coordinates describing the motion of the system. The lack of constraint equations has a great influence on efficient integration of equations of motion. When closed loops are included in the system, additional difficulties occur. The relatively complex constraint equations have to be formulated and it is difficult to generalize those constraints for all cases. Despite such problems, this method has been applied by some authors. Kim [19] used joint coordinates in dynamic analysis of vehicle motion. Authors of papers [20] and [21] applied homogeneous transformations and joint coordinates to create simple models of passenger vehicles and articulated lorries. The approach presented there is based on the work performed by Denavit and Hartenberg [22] and books [23, 24].

The papers mentioned above present small car models for which the number of degrees of freedom does not exceed 20. In this paper, we present a model which includes some new flexible elements such as shock absorbers (characterized by longitudinal flexibility) and shafts, semi-axles and steering columns (characterized by torsional flexibility). Moreover, a general approach that enables us to involve such elements into the system is described. The correctness of models and algorithms formulated is verified by comparison of numerical results obtained with those obtained by application of commercial package and experimental measurements.

In this paper, joint coordinates and homogeneous transformations are applied to describing the motion of a passenger car, taking into account a structural model of suspensions.

## 2 General description of the method

Displacement of a body in space requires two operations: translation and rotation. Let us assume two coordinate systems: the local one designated as $\{\}'$, which is rigidly attached to the body considered, and the reference frame designated as $\{\}$, which can be an inertial coordinate system (Fig. 1(a)). The position of the body is defined when the following are known: the vector $\mathbf{r}_0$ defining the coordinates of the origin of system $\{\}'$ with respect to $\{\}$, and the rotation matrix $\mathbf{R}$ defining the orientation of $\{\}'$ in $\{\}$. In order to describe the orientation of frame $\{\}'$, we apply the parameters called Euler angles ZYX [25] (Fig. 1(b)). The rotation matrix $\mathbf{R}$ parameterized by ZYX Euler angles has the form:

$$\mathbf{R} = \begin{bmatrix} c\psi & -s\psi & 0 \\ s\psi & c\psi & 0 \\ 0 & 0 & 1 \end{bmatrix} \begin{bmatrix} c\theta & 0 & s\theta \\ 0 & 1 & 0 \\ -s\theta & 0 & c\theta \end{bmatrix} \times \begin{bmatrix} 1 & 0 & 0 \\ 0 & c\varphi & -s\varphi \\ 0 & s\varphi & c\varphi \end{bmatrix}$$

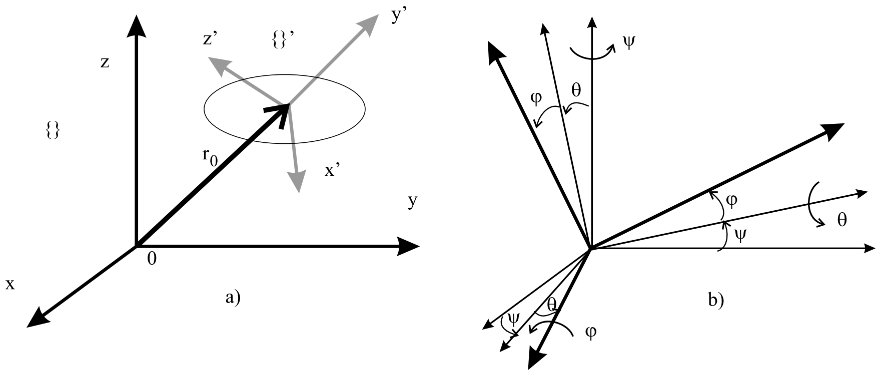


**Fig. 1** Coordinate systems and ZYX Euler angles. **a** Global (reference) frame { } and local frame { }′, **b** ZYX Euler angles $\psi, \theta, \varphi$

$$= \begin{bmatrix} c\psi c\theta & c\psi s\theta s\varphi - s\psi c\varphi & c\psi s\theta c\varphi + s\psi s\varphi \\ s\psi c\theta & s\psi s\theta s\varphi + c\psi c\varphi & s\psi s\theta c\varphi - c\psi s\varphi \\ -s\theta & c\theta s\varphi & c\theta c\varphi \end{bmatrix} \tag{1}$$

where $s\psi = \sin(\psi)$, $s\theta = \sin(\theta)$, $s\varphi = \sin(\varphi)$, $c\psi = \cos(\psi)$, $c\theta = \cos(\theta)$, $c\varphi = \cos(\varphi)$.

The transformation of coordinates from local system $\{\}'$ to global $\{\}$ can be performed according to the formula:

$$\mathbf{r} = \mathbf{R} \cdot \mathbf{r}' + \mathbf{r}_0 \tag{2}$$

where $\mathbf{r}' = [x' \;\; y' \;\; z']^T$ and $\mathbf{r} = [x \;\; y \;\; z]^T$ are respectively the coordinates of any point in local and global coordinate systems.

The transformation defined by (2) requires two mathematical operations: multiplication of the matrix by the vector and summation of vectors. The homogeneous transformations [23, 24] enable the transformation of coordinates to be presented by means of only one operation: multiplication of a matrix by vector:

$$\bar{\mathbf{r}} = \mathbf{T} \cdot \bar{\mathbf{r}}' \tag{3}$$

where

$$\bar{\mathbf{r}} = \begin{bmatrix} \mathbf{r} \\ 1 \end{bmatrix} = [x \quad y \quad z \quad 1]^T,$$

$$\bar{\mathbf{r}}' = \begin{bmatrix} \mathbf{r}' \\ 1 \end{bmatrix} = [x' \quad y' \quad z' \quad 1]^T,$$

$$\mathbf{T} = \begin{bmatrix} \mathbf{R} & \mathbf{r}_0 \\ \mathbf{0} & 1 \end{bmatrix}.$$

In further considerations, the bar ¯ will be omitted, and homogeneous coordinates and transformation will be applied, except for some indicated cases. Matrix $\mathbf{T}$ from the above formulae can also be presented in the form:

$$\mathbf{T} = \prod_{i=1}^{6} \mathbf{T}_i \tag{4}$$

where

$$\mathbf{T}_1 = \mathbf{T}_1(x_0) = \begin{bmatrix} 1 & 0 & 0 & x_0 \\ 0 & 1 & 0 & 0 \\ 0 & 0 & 1 & 0 \\ 0 & 0 & 0 & 1 \end{bmatrix},$$

$$\mathbf{T}_2 = \mathbf{T}_2(y_0) = \begin{bmatrix} 1 & 0 & 0 & 0 \\ 0 & 1 & 0 & y_0 \\ 0 & 0 & 1 & 0 \\ 0 & 0 & 0 & 1 \end{bmatrix},$$

$$\mathbf{T}_3 = \mathbf{T}_3(z_0) = \begin{bmatrix} 1 & 0 & 0 & 0 \\ 0 & 1 & 0 & 0 \\ 0 & 0 & 1 & z_0 \\ 0 & 0 & 0 & 1 \end{bmatrix},$$

$$\mathbf{T}_4 = \mathbf{T}_4(\psi) = \begin{bmatrix} c\psi & -s\psi & 0 & 0 \\ s\psi & c\psi & 0 & 0 \\ 0 & 0 & 1 & 0 \\ 0 & 0 & 0 & 1 \end{bmatrix},$$

$$\mathbf{T}_5 = \mathbf{T}_5(\theta) = \begin{bmatrix} c\theta & 0 & s\theta & 0 \\ 0 & 1 & 0 & 0 \\ -s\theta & 0 & c\theta & 0 \\ 0 & 0 & 0 & 1 \end{bmatrix},$$

$$\mathbf{T}_6 = \mathbf{T}_6(\varphi) = \begin{bmatrix} 1 & 0 & 0 & 0 \\ 0 & c\varphi & -s\varphi & 0 \\ 0 & s\varphi & c\varphi & 0 \\ 0 & 0 & 0 & 1 \end{bmatrix}.$$

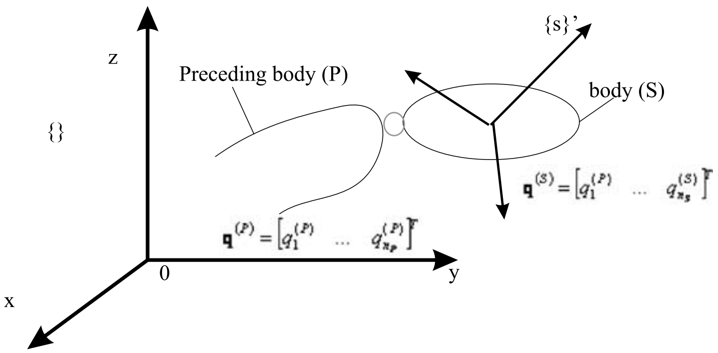


**Fig. 2** The body $(S)$ attached to preceding body $(P)$. Vectors $\mathbf{q}^{(P)}$ and $\mathbf{q}^{(S)}$ are generalized coordinates describing motion of bodies $(P)$ and $(S)$, respectively

It can be seen that each matrix $\mathbf{T}_1$ to $\mathbf{T}_6$ depends on only one parameter. In several dynamic problems, some components of the vector:

$$\tilde{\mathbf{q}} = [x_0 \quad y_0 \quad z_0 \quad \psi \quad \theta \quad \varphi]^T \tag{5}$$

describing body motion can be assumed to be constant or known, and the number of degrees of freedom of a body becomes less than 6.

Figure 2 presents two connected bodies: $(P)$ and $(S)$. It is assumed that the motion of body $(P)$ (preceding body), and the relative motion of body $(S)$, are described by the components of the following vectors:

$$\mathbf{q}^{(P)} = \begin{bmatrix} q_1^{(P)} & \dots & q_{n_P}^{(P)} \end{bmatrix}^T \tag{6a}$$

$$\tilde{\mathbf{q}}^{(S)} = \begin{bmatrix} \tilde{q}_1^{(S)} & \dots & \tilde{q}_{\tilde{n}_S}^{(S)} \end{bmatrix}^T \tag{6b}$$

where $\tilde{n}_S \le 6$ is the number of degrees of freedom of body (S) in relative motion, $\tilde{q}_1^S, \dots, \tilde{q}_{\tilde{n}_S}^{(S)}$ are components of vector (5) defining the relative motion of body (S) in relation to the preceding body $(P)$.

Thus, the vector of generalized coordinates of body $(S)$ can be written as follows:

$$\mathbf{q}^{(S)} = \begin{bmatrix} \mathbf{q}^{(P)} \\ \tilde{\mathbf{q}}^{(S)} \end{bmatrix} = \begin{bmatrix} q_1^{(S)} & \dots & q_{n_S}^{(S)} \end{bmatrix}^T \tag{7}$$

where $n_S = n_P + \tilde{n}_S$,

$$\mathbf{q}_i^{(S)} = \begin{cases} \mathbf{q}_i^{(P)}, & \text{for } i \le n_P, \\ \tilde{\mathbf{q}}_{i-n_P}, & \text{for } i = n_P + 1, \dots, n_P + \tilde{n}_S. \end{cases}$$

It is also assumed that the transformation matrix of coordinates from local coordinate system $\{P\}'$ to inertial coordinate system $\{\}$ can be designated as $\mathbf{B}^{(P)}(\mathbf{q}^{(P)})$, and the transformation matrix from local frame $\{S\}'$ to frame $\{P\}'$ of preceding body $(P)$ is designated as $\mathbf{T}^{(P)}(\tilde{\mathbf{q}}^{(S)})$. Now the coordinates from local coordinate system $\{S\}'$ can be transformed to inertial coordinate system $\{\}$ according to the formula:

$$\mathbf{r}^{(S)} = \mathbf{B}^{(P)}\big(\mathbf{q}^{(P)}\big)\mathbf{T}^{(S)}\big(\tilde{\mathbf{q}}^{(S)}\big)\mathbf{r}'^{(S)} = \mathbf{B}^{(S)}\big(\mathbf{q}^{(S)}\big)\mathbf{r}'^{(S)} \tag{8}$$

where $\mathbf{B}^{(S)} = \mathbf{B}^{(P)} \cdot \mathbf{T}^{(S)}$.

The equations of motion of body $(S)$ can be formulated using Lagrange equations:

$$\frac{d}{dt}\frac{\partial E^{(S)}}{\partial \dot{\mathbf{q}}_k^{(S)}} - \frac{\partial E^{(S)}}{\partial \mathbf{q}_k^{(S)}} + \frac{\partial V^{(S)}}{\partial \mathbf{q}_k^{(S)}} = \mathbf{Q}_k^{(S)} \tag{9}$$

where $k = 1, \dots, n_S$, functionals $E^{(S)}$ and $V^{(S)}$ define kinetic and potential energy of body $(S)$, $\mathbf{Q}_k^{(S)}$ are non-potential generalized forces, $\mathbf{q}_k^{(S)}$ and $\dot{\mathbf{q}}_k^{(S)}$ are generalized coordinates and velocities of body $(S)$.

## 2.1 Kinetic energy

In order to calculate the kinetic energy, the following relation is used:

$$v^2 = \dot{x}^2 + \dot{y}^2 + \dot{z}^2 = \operatorname{tr}\left\{\begin{bmatrix} \dot{x}^2 & \dot{x}\dot{y} & \dot{x}\dot{z} & 0 \\ \dot{x}\dot{y} & \dot{y}^2 & \dot{z}\dot{y} & 0 \\ \dot{x}\dot{z} & \dot{y}\dot{z} & \dot{z}^2 & 0 \\ 0 & 0 & 0 & 0 \end{bmatrix}\right\}$$

$$= \operatorname{tr}\left\{\begin{bmatrix} \dot{x} \\ \dot{y} \\ \dot{z} \\ 0 \end{bmatrix} [\dot{x} \quad \dot{y} \quad \dot{z} \quad 0]\right\} = \operatorname{tr}\big\{\dot{\mathbf{r}} \cdot \dot{\mathbf{r}}^T\big\} \tag{10}$$

where $\mathbf{r} = [x \ y \ z \ 1]^T$, $\operatorname{tr}\{\mathbf{A}\} = \sum_{i=1}^4 a_{ii}$ is the trace of matrix $\mathbf{A}$.

Using formulae (10) and (8) the kinetic energy of body $(S)$ can be calculated as:

$$E^{(S)} = \frac{1}{2}\int_{m^{(S)}} \operatorname{tr}\big\{\dot{\mathbf{r}}^{(S)}\dot{\mathbf{r}}^{(S)^T}\big\}\, dm^{(S)}$$

$$
\begin{aligned}
&= \frac{1}{2}\int_{m^{(S)}} \operatorname{tr}\{\dot{\mathbf{B}}^{(S)}\mathbf{r}'^{(S)}[\dot{\mathbf{B}}^{(S)}\mathbf{r}'^{(S)}]^T\}\, dm^{(S)} \\
&= \frac{1}{2}\operatorname{tr}\left\{\dot{\mathbf{B}}^{(S)}\left[\int_{m^{(S)}} \mathbf{r}'^{(S)}\mathbf{r}'^{(S)^T}\, dm^{(S)}\right]\dot{\mathbf{B}}^{(S)^T}\right\} \\
&= \frac{1}{2}\operatorname{tr}\{\dot{\mathbf{B}}^{(S)}\mathbf{H}^{(S)}\dot{\mathbf{B}}^{(S)^T}\}
\end{aligned}
\tag{11}
$$

where $m^{(S)}$ is the mass of body $(S)$,

$$
\begin{aligned}
\mathbf{H}^{(S)} &= \int_{m^{(S)}} \mathbf{r}'^{(S)}\mathbf{r}'^{(S)^T} \\
&= \int_{m^{(S)}} \begin{bmatrix} x'^{(S)}x'^{(S)} & x'^{(S)}y'^{(S)} & x'^{(S)}z'^{(S)} & x'^{(S)} \\ y'^{(S)}x'^{(S)} & y'^{(S)}y'^{(S)} & y'^{(S)}z'^{(S)} & y'^{(S)} \\ z'^{(S)}x'^{(S)} & z'^{(S)}y'^{(S)} & z'^{(S)}z'^{(S)} & z'^{(S)} \\ x'^{(S)} & y'^{(S)} & z'^{(S)} & 1 \end{bmatrix} \\
&\quad \times dm^{(S)}.
\end{aligned}
$$

Matrix $\mathbf{H}^{(S)}$ is a pseudo-inertia matrix and its elements can be expressed in the forms:

$$
\begin{aligned}
&\begin{cases}
\mathbf{H}_{11}^{(S)} = \frac{1}{2}[-I_x^{(S)} + I_y^{(S)} + I_z^{(S)}], \\
\mathbf{H}_{22}^{(S)} = \frac{1}{2}[I_x^{(S)} - I_y^{(S)} + I_z^{(S)}], \\
\mathbf{H}_{33}^{(S)} = \frac{1}{2}[I_x^{(S)} + I_y^{(S)} - I_z^{(S)}],
\end{cases} \\
&\begin{cases}
\mathbf{H}_{12}^{(S)} = \mathbf{H}_{21}^{(S)} = I_{xy}^{(S)}, \\
\mathbf{H}_{13}^{(S)} = \mathbf{H}_{31}^{(S)} = I_{xz}^{(S)}, \\
\mathbf{H}_{32}^{(S)} = \mathbf{H}_{23}^{(S)} = I_{yz}^{(S)},
\end{cases} \\
&\begin{cases}
\mathbf{H}_{14}^{(S)} = \mathbf{H}_{41}^{(S)} = m^{(S)}x_c'^{(S)}, \\
\mathbf{H}_{24}^{(S)} = \mathbf{H}_{42}^{(S)} = m^{(S)}y_c'^{(S)}, \\
\mathbf{H}_{34}^{(S)} = \mathbf{H}_{43}^{(S)} = m^{(S)}z_c'^{(S)}, \\
\mathbf{H}_{44}^{(S)} = m^{(S)}
\end{cases}
\end{aligned}
\tag{12}
$$

where $I_x^{(S)}$, $I_y^{(S)}$, $I_z^{(S)}$ are moments of inertia of body $(S)$ with respect to local axes $x'^{(S)}$, $y'^{(S)}$, $z'^{(S)}$; $I_{xy}^{(S)}$, $I_{xz}^{(S)}$, $I_{yz}^{(S)}$ are products of inertia with respect to local coordinate system $\{S\}'$; $x_c'^{(S)}$, $y_c'^{(S)}$, $z_c'^{(S)}$ are coordinates of the center of mass of body $(S)$ in the local coordinate system.

Matrix $\mathbf{H}^{(S)}$ is a symmetric matrix with constant coefficients and becomes diagonal when the axes of the local coordinate system $\{S\}'$ coincide with the principal-central inertial axes of body $(S)$.

If we assume, that matrix $\mathbf{B}$ does not depend directly on time $t$, then we obtain:

$$
\dot{\mathbf{B}}^{(S)} = \frac{d\mathbf{B}^{(S)}}{dt} = \sum_{i=1}^{n_S} \mathbf{B}_i^{(S)}\dot{q}_i^{(S)} \tag{13}
$$

where $\mathbf{B}_i^{(S)} = \frac{\partial \mathbf{B}^{(S)}}{\partial q_i^{(S)}}$.

From (11) after some transformations it is possible to calculate:

$$
\varepsilon_k^{(S)} = \frac{d}{dt}\frac{\partial E^{(S)}}{\partial \dot{q}_k^{(S)}} - \frac{\partial E^{(S)}}{\partial q_k^{(S)}} = \operatorname{tr}\{\mathbf{B}_k^{(S)}\mathbf{H}^{(S)}\ddot{\mathbf{B}}^{(S)^T}\} \tag{14}
$$

for $k = 1, \dots, n_S$.

Differentiating (13), we obtain:

$$
\ddot{\mathbf{B}}^{(S)} = \sum_{i=1}^{n_S} \mathbf{B}_i^{(S)}\ddot{q}_i^{(S)} + \sum_{i=1}^{n_S}\sum_{j=1}^{n_S} \mathbf{B}_{ij}^{(S)}\dot{q}_i^{(S)}\dot{q}_j^{(S)} \tag{15}
$$

where $\mathbf{B}_{ij}^{(S)} = \frac{\partial \mathbf{B}_i^{(S)}}{\partial q_j^{(S)}} = \frac{\partial^2 \mathbf{B}^{(S)}}{\partial q_i^{(S)} q_j^{(S)}}$, and formulae (14) can be written in the form:

$$
\varepsilon_k^{(S)} = \sum_{i=1}^{n_S} a_{ki}^{(S)}\ddot{q}_i^{(S)} + \sum_{i=1}^{n_S}\sum_{j=1}^{n_S} b_{kij}^{(S)}\dot{q}_i^{(S)}\dot{q}_j^{(S)} \tag{16}
$$

where

$$
a_{ki}^{(S)} = \operatorname{tr}\{\mathbf{B}_k^{(S)}\mathbf{H}^{(S)}\mathbf{B}_i^{(S)^T}\},
$$

$$
b_{kij}^{(S)} = \operatorname{tr}\{\mathbf{B}_k^{(S)}\mathbf{H}^{(S)}\mathbf{B}_{ij}^{(S)^T}\},
$$

or equivalently:

$$
\begin{aligned}
\epsilon_{\mathbf{q}^{(S)}}(E^{(S)}) &= \frac{d}{dt}\frac{\partial}{\partial \dot{\mathbf{q}}^{(S)}}(E^{(S)}) \\
&= \mathbf{A}^{(S)}\ddot{\mathbf{q}}^{(S)} + \mathbf{h}^{(S)}
\end{aligned}
\tag{17}
$$

where

$$
\mathbf{A}^{(S)} = (a_{ki}^{(S)})_{k,i=1,\dots,n_S}, \qquad \mathbf{h}^{(S)} = (h_k^{(S)})_{k=1,\dots,n_S},
$$

$$
h_k^{(S)} = \sum_{i=1}^{n_S}\sum_{j=1}^{n_S} b_{kij}^{(S)}\dot{q}_i^{(S)}\dot{q}_j^{(S)}.
$$

### 2.2 Potential energy of gravity forces

The coordinates of the center of mass of body $(S)$ can be expressed in local frame $\{S\}'$ according to (12) as:

$$
\mathbf{r}_c'^{(S)} = \begin{bmatrix} x_c'^{(S)} & y_c'^{(S)} & z_c'^{(S)} & 1 \end{bmatrix}^T \tag{18}
$$

and its coordinates in the inertial frame are calculated as follows:

$$\mathbf{r}_c^{(S)} = \mathbf{B}^{(S)} \mathbf{r}_c^{\prime(S)}. \tag{19}$$

When axis $z$ of the inertial coordinate system $\{\}$ is perpendicular to the earth's surface, the following can be written:

$$V_g^{(S)} = m^{(S)} g \cdot z_c^{(S)} \tag{20}$$

where $g$ is the acceleration of gravity, $z_c^{(S)}$ is the third coordinate of the center of mass in inertial frame $\{\}$. The coordinate $z_c^{(S)}$ can be calculated as

$$z_c^{(S)} = \theta_3 \mathbf{B}^{(S)} \mathbf{r}_c^{\prime(S)} \tag{21}$$

where $\theta_3 = [0\ 0\ 1\ 0]$.

From the above formulae we obtain:

$$V_g^{(S)} = m^{(S)} g \theta_3 \mathbf{B}^{(S)} \mathbf{r}_c^{\prime(S)}, \tag{22a}$$

$$\frac{\partial V_g^{(S)}}{q_k^{(S)}} = m^{(S)} g \theta_3 \mathbf{B}_k^{(S)} \mathbf{r}^{\prime(S)} \tag{22b}$$

or in vector form:

$$\frac{\partial \mathbf{V}_g^{(S)}}{\partial \mathbf{q}^{(S)}} = \mathbf{F}_g^{(S)} \tag{22c}$$

where

$$\mathbf{F}_g^{(S)} = \left( \frac{\partial \mathbf{V}_g^{(S)}}{\partial \mathbf{q}_k^{(S)}} \right)_{k=1,\dots,n_S}.$$

## 2.3 Generalized forces

External forces and moments acting on body $(S)$ have to be included in (9) by means of generalized forces. Figure 3 presents force $\mathbf{P}'$ and moment $\mathbf{M}'$, defined in the local frame, acting on body $(S)$. Vectors $\mathbf{P}^{\prime(S)}$ and $\mathbf{M}^{\prime(S)}$ have the forms:

$$\mathbf{P}^{\prime(S)} = \begin{bmatrix} P_x^{\prime(S)} & P_y^{\prime(S)} & P_y^{\prime(S)} & 0 \end{bmatrix}^T, \tag{23a}$$

$$\mathbf{M}^{\prime(S)} = \begin{bmatrix} M_x^{\prime(S)} & M_y^{\prime(S)} & M_y^{\prime(S)} & 0 \end{bmatrix}^T \tag{23b}$$

(the fourth component is equal to 0).

Proceeding as in [20], one can obtain the generalized forces caused by $\mathbf{P}^{\prime(S)}$ and $\mathbf{M}^{\prime(S)}$

$$\mathbf{Q}_k\left(\mathbf{P}^{\prime(S)}\right) + \mathbf{Q}_k\left(\mathbf{M}^{\prime(S)}\right) = \mathbf{P}^{\prime(S)^T} \mathbf{r}_{A,k}^{\prime(S)} + \mathbf{M}^{\prime(S)^T} \mathbf{d}_k^{\prime(S)} \tag{24}$$

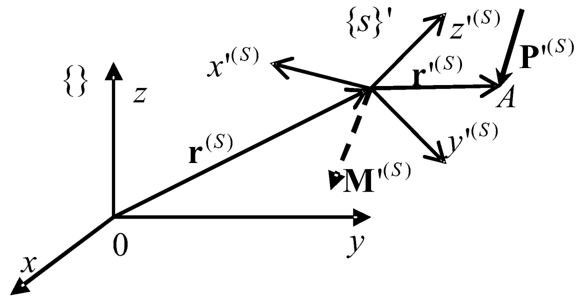


**Fig. 3** Force $\mathbf{P}'$ and moment $\mathbf{M}'$ defined in local frame $\{S\}'$

where

$$\mathbf{r}_{A,k}^{\prime(S)} = \mathbf{B}^{(S)^T} \mathbf{B}_k^{(S)} \mathbf{r}_A^{\prime(S)},$$

$$\mathbf{d}_k^{\prime(S)} = \begin{bmatrix} d_{k1}^{\prime(S)} & d_{k2}^{\prime(S)} & d_{k3}^{\prime(S)} \end{bmatrix}^T,$$

$$d_{k1}^{\prime(S)} = \sum_{l=1}^{3} b_{l3}^{(S)} b_{kl2}^{(S)}, \qquad d_{k2}^{\prime(S)} = \sum_{l=1}^{3} b_{l1}^{(S)} b_{kl3}^{(S)},$$

$$d_{k3}^{\prime(S)} = \sum_{l=1}^{3} b_{l2}^{(S)} b_{kl1}^{(S)},$$

$$\left(b_{lj}^{(S)}\right)_{l,j=1,2,3}, \left(b_{klj}^{(S)}\right)_{k=1,\dots,n_S;l,j=1,2,3}$$

are respectively the elements of matrices $\mathbf{B}^{(S)}$ and $\mathbf{B}_k^{(S)}$.

Bearing in mind formulae (17), (22c) and (24), the equations of motion of body $(S)$ can be written in the form:

$$\mathbf{A}^{(S)} \ddot{\mathbf{q}}^{(S)} = \mathbf{Q}^{(S)} - \mathbf{h}^{(S)} - \mathbf{F}_g^{(S)} = \mathbf{f}^{(S)} \tag{25}$$

where $\mathbf{A}^{(S)}$, $\mathbf{h}^{(S)}$, $\mathbf{F}_g^{(S)}$ are defined in (17), (22c), $\mathbf{Q}^{(S)} = (\mathbf{Q}_k^{(S)})_{k=1,\dots,n_S}$, and $\mathbf{Q}_k^{(S)}$ are defined in (25).

Taking into account definition (7), it is possible to write (25) in the form:

$$\begin{bmatrix} \mathbf{A}_{pp}^{(S)} & \mathbf{A}_{ps}^{(S)} \\ \mathbf{A}_{sp}^{(S)} & \mathbf{A}_{ss}^{(S)} \end{bmatrix} \begin{bmatrix} \ddot{\mathbf{q}}^{(P)} \\ \ddot{\tilde{\mathbf{q}}}^{(S)} \end{bmatrix} = \begin{bmatrix} \mathbf{h}_p^{(S)} - \mathbf{F}_{g,p}^{(S)} - \mathbf{Q}_p^{(S)} \\ \mathbf{h}_s^{(S)} - \mathbf{F}_{g,s}^{(S)} - \mathbf{Q}_s^{(S)} \end{bmatrix} = \begin{bmatrix} \mathbf{f}_p^{(S)} \\ \mathbf{f}_s^{(S)} \end{bmatrix} \tag{26}$$

where

$$\mathbf{A}_{pp}^{(S)} = \left(a_{ki}^{(S)}\right)_{k,i=1,\dots,n_P},$$

$$\mathbf{A}_{ps}^{(S)} = \mathbf{A}_{ap}^{(S)^T} = \left(a_{ki}^{(S)}\right)_{\substack{k,i=1,\dots,n_P \\ i=n_P+1,\dots,n_P+\tilde{n}_S}},$$

$$\mathbf{A}_{ss}^{(S)} = \left(a_{ki}^{(S)}\right)_{k,i=n_P+1,\ldots,n_P+\tilde{n}_S},$$

$$\mathbf{h}_p^{(S)} = \left(h_k^{(S)}\right)_{k=1,\ldots,n_P}, \qquad \mathbf{h}_s^{(S)} = \left(h_k^{(S)}\right)_{k=n_P+1,\ldots,\tilde{n}_S},$$

$$\mathbf{F}_{g,p}^{(S)} = \left(\frac{\partial V_g^{(S)}}{\partial q_k^{(P)}}\right)_{k=1,\ldots,n_P},$$

$$\mathbf{F}_{g,s}^{(S)} = \left(\frac{\partial V_g^{(S)}}{\partial \tilde{q}_k^{(S)}}\right)_{k=1,\ldots,\tilde{n}_S},$$

$$\mathbf{Q}_p^{(S)} = \left(Q_k^{(S)}\right)_{k=1,\ldots,n_P},$$

$$\mathbf{Q}_s^{(S)} = \left(Q_k^{(S)}\right)_{k=n_P+1,\ldots,n_P+\tilde{n}_S}.$$

Equations (26) show how the equations of motion of body $(S)$ depend on the generalized coordinates of the preceding body $\mathbf{q}^{(P)}$ and vector $\tilde{\mathbf{q}}^{(S)}$. It is also possible to demonstrate how body $(S)$, when attached to the preceding chain, changes the equations of motion of this chain. If it is assumed that the equations of motion of preceding bodies have the form:

$$\tilde{\mathbf{A}}^{(P)}\ddot{\mathbf{q}}^{(P)} = \tilde{\mathbf{f}}^{(P)} \tag{27}$$

then the equations of motion of the system, including the preceding chain and body $(S)$, can be written in the form:

$$\tilde{\mathbf{A}}^{(S)}\ddot{\mathbf{q}}^{(S)} = \tilde{\mathbf{f}}^{(S)} \equiv \begin{bmatrix} \mathbf{A}^{(P)} + \mathbf{A}_{pp}^{(S)} & \mathbf{A}_{ps}^{(S)} \\ \mathbf{A}_{sp}^{(S)} & \mathbf{A}_{ss}^{(S)} \end{bmatrix} \begin{bmatrix} \ddot{\mathbf{q}}^{(P)} \\ \ddot{\tilde{\mathbf{q}}}^{(S)} \end{bmatrix} = \begin{bmatrix} \mathbf{f}^{(P)} + \mathbf{f}_p^{(S)} \\ \mathbf{f}_s^{(S)} \end{bmatrix}. \tag{28}$$

It should be stressed that the connection of body $(S)$ modifies the equations of motion of preceding bodies. This is an essential feature of using joint coordinates.

## 3 Flexible elements and constraint equations

When dynamics of a multibody are considered, some special spring-damping elements (such as shock absorbers or flexible axles) have to be taken into account. It is also necessary to analyze connections between subsystems which provide joint reactions and constraint equations. Considerations below allow us to formulate models of spring damping elements and models of joints using homogeneous transformations.

Commercial packages usually use the finite element method for modeling of flexible links. Then, modal analysis is necessary for the reduction of the number of generalized coordinates. In our work, we use the rigid finite element method for discretization of flexible elements. The formulation of this method when joint coordinates and $4 \times 4$ transformation matrices are used is presented in [26]. Formulation of modal method adapted for rigid-flexible structures can be found in [21] together with its multiplicative forms of transformation matrices.

### 3.1 Model of a shock absorber

It is assumed that a shock absorber connects bodies $(N)$ and $(P)$, which belong to two different subchains with a common (base) body designated by $(L)$ in Fig. 4. The energy of spring deformation of the shock absorber and the dissipation of its energy can be expressed as follows:

$$\mathbf{V}^{(N,P)} = \frac{1}{2}k^{(N,P)}\left[\Delta\mathbf{r}_{AB}^{(L)}\right]^T \Delta\mathbf{r}_{AB}^{(L)}, \tag{29a}$$

$$\mathbf{D}^{(N,P)} = \frac{1}{2}c^{(N,P)}\left[\Delta\dot{\mathbf{r}}_{CD}^{(L)}\right]^T \Delta\dot{\mathbf{r}}_{CD}^{(L)} \tag{29b}$$

where $k^{(N,P)}$, $c^{(N,P)}$ are stiffness and damping coefficients, $\Delta\mathbf{r}_{AB}^{(L)}$ and $\Delta\dot{\mathbf{r}}_{CD}^{(L)}$ are spring deformations and deformation velocity, respectively.

The spring deformation and its velocity can be calculated with respect to base body (L) as follows:

$$\Delta\mathbf{r}_{AB}^{(L)} = \mathbf{r}_A^{(L)} - \mathbf{r}_B^{(L)} - \Delta\mathbf{r}_{AB,0}^{(L)}, \tag{30a}$$

$$\Delta\dot{\mathbf{r}}_{CD}^{(L)} = \dot{\mathbf{r}}_C^{(L)} - \dot{\mathbf{r}}_D^{(L)} \tag{30b}$$

where $\mathbf{r}_A^{(L)}$, $\mathbf{r}_A^{(L)}$ are vectors of coordinates of points $A$, $B$, $\Delta\mathbf{r}_{AB,0}^{(L)} = \Delta\mathbf{r}_{AB}^{(L)}$ in the case when spring is not deformed, $\dot{\mathbf{r}}_L^{(L)}$, $\dot{\mathbf{r}}_L^{(D)}$ are velocities of points $C$ and $D$, respectively.

Assuming that the transformation matrices from body $(N)$ to $(L)$ and from $(P)$ to $(L)$ are as follows:

$$\mathbf{B}^{(L,N)} = \mathbf{B}^{(L,N)}\left(\mathbf{q}^{(L,N)}\right), \tag{31a}$$

$$\mathbf{B}^{(L,P)} = \mathbf{B}^{(L,P)}\left(\mathbf{q}^{(L,P)}\right) \tag{31b}$$

where

$$\mathbf{q}^{(L,N)} = \left[q_1^{(L,N)} \quad \ldots \quad q_{\tilde{n}^{(L,N)}}^{(L,N)}\right]^T,$$

$$\mathbf{q}^{(L,P)} = \left[q_1^{(L,P)} \quad \ldots \quad q_{\tilde{n}^{(L,P)}}^{(L,P)}\right]^T$$

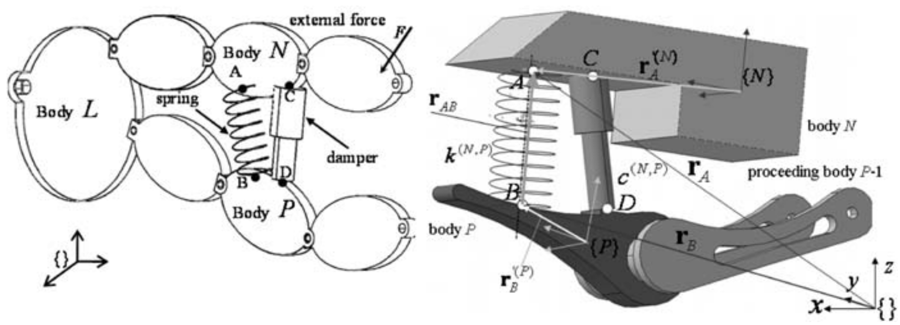


**Fig. 4** Flexible connection between bodies $(P)$ and $(N)$

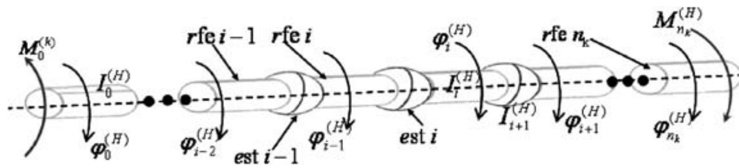


**Fig. 5** Discretized flexible shaft

are the vectors of generalized coordinates defining relative motion of bodies $(N)$ and $(P)$ with respect to base body $(L)$, it is possible to calculate:

$$\mathbf{r}_A^{(L)} = \mathbf{B}^{(L,N)}\mathbf{r}_A'^{(N)}, \tag{32a}$$

$$\mathbf{r}_B^{(L)} = \mathbf{B}^{(L,P)}\mathbf{r}_B'^{(P)} \tag{32b}$$

and

$$\dot{\mathbf{r}}_C^{(L)} = \dot{\mathbf{B}}^{(L,N)}\mathbf{r}_C'^{(N)}, \tag{33a}$$

$$\dot{\mathbf{r}}_D^{(L)} = \dot{\mathbf{B}}^{(L,P)}\mathbf{r}_D'^{(P)} \tag{33b}$$

where $\mathbf{r}_A'^{(N)}$, $\mathbf{r}_C'^{(N)}$, $\mathbf{r}_B'^{(P)}$, $\mathbf{r}_D'^{(P)}$ are vectors of coordinates of points $A$, $C$ and $B$, $D$ in local frame $\{N\}'$, $\{P\}'$ of body $(N)$ and $(P)$, respectively.

From the above we can obtain

$$\frac{\partial V^{(N,P)}}{\partial q_j^{(L,N)}} = k^{(N,P)}\Delta\mathbf{r}_{AB}^{(L)^T}\mathbf{B}_j^{(L,N)}\mathbf{r}_A'^{(N)}, \tag{34a}$$

$$\frac{\partial D^{(N,P)}}{\partial \dot{q}_j^{(L,N)}} = c^{(N,P)}\Delta\dot{\mathbf{r}}_{CD}^{(L)^T}\mathbf{B}_j^{(L,N)}\mathbf{r}_C'^{(N)} \tag{34b}$$

for $j = 1, \ldots, \tilde{n}_{L,N}$,

$$\frac{\partial V^{(N,P)}}{\partial q_j^{(L,P)}} = -k^{(N,P)}\Delta\mathbf{r}_{AB}^{(L)^T}\mathbf{B}_j^{(L,P)}\mathbf{r}_B'^{(N)}, \tag{35a}$$

$$\frac{\partial D^{(N,P)}}{\partial \dot{q}_j^{(L,P)}} = -c^{(N,P)}\Delta\dot{\mathbf{r}}_{CD}^{(L)^T}\mathbf{B}_j^{(L,P)}\mathbf{r}_D'^{(N)} \tag{35b}$$

for $j = 1, \ldots, \tilde{n}_{L,P}$.

The above terms have to be added to the equations of motion relevant to the generalized coordinates defined by vectors $\mathbf{q}^{(L,N)}$ and $\mathbf{q}^{(L,P)}$.

## 3.2 Model of elements with torsional flexibility

Another type of elements frequently used in modeling of car dynamics are shafts, semi-axles and steering columns characterized by torsional flexibility.

It is assumed that the subsystem presented in Fig. 5 can be divided into rigid finite elements (rfe) numbered from 0 to $\tilde{n}^{(H)}$, and connected by massless and non-dimensional spring-damping elements (sde) numbered from 1 to $\tilde{n}^{(H)}$. The kinetic energy of the subsystem can be expressed, according to [26], as follows:

$$\mathbf{T}^{(H)} = \frac{1}{2}\sum_{i=0}^{\tilde{n}^{(H)}} I_i^{(H)}\left(\dot{\varphi}_i^{(H)}\right)^2 \tag{36}$$

where $I_i^{(H)}$ are mass moments of inertia of rfe 0–$\tilde{n}^{(H)}$, $\varphi_i^{(H)}$ are rotation angles of rfes.

The potential energy of deformation of (sde) 1–$\tilde{n}^{(H)}$ and the energy of dissipation can be written in the forms:

$$V^{(H)} = \frac{1}{2}\sum_{i=1}^{\tilde{n}^{(H)}} k_i^{(H)}\left[\varphi_i^{(H)} - \varphi_{i-1}^{(H)}\right]^2, \tag{37a}$$

$$D^{(H)} = \frac{1}{2}\sum_{i=1}^{\tilde{n}^{(H)}} c_i^{(H)}\left[\dot{\varphi}_i^{(H)} - \dot{\varphi}_{i-1}^{(H)}\right]^2 \tag{37b}$$

where $k_i^{(H)}$ and $c_i^{(H)}$ are stiffness and damping coefficients of sde $i$.

Taking expressions (36) and (37) into account, one can obtain the equations of motion of subsystem $(H)$ in the form:

$$\mathbf{A}^{(H)}\ddot{\mathbf{q}}^{(H)} = \mathbf{f}^{(H)} \tag{38}$$

where $\mathbf{q}^{(H)} = [\varphi_0^{(H)} \ \dots \ \varphi_{\tilde{n}^{(H)}}]^T$, $\mathbf{A}^{(H)}$ is a diagonal mass matrix with constant coefficients, $\mathbf{f}^{(H)} = \mathbf{Q}^{(H)} - \mathbf{K}^{(H)}\mathbf{q}^{(H)} - \mathbf{C}^{(H)}\dot{\mathbf{q}}^{(H)}$, $\mathbf{Q}^{(H)}$ is the vector of generalized (not potential) forces, $\mathbf{K}^{(H)}$ and $\mathbf{C}^{(C)}$ are matrices with constant coefficients.

The components of vector $\mathbf{Q}^{(H)}$ depend on moments $M_0^{(H)}$ and $M_{\tilde{n}^{(H)}}^{(H)}$, which could be external torques, or internal reaction moments in the case when element $(H)$ connects bodies $(N)$ and $(P)$. In the second case the appropriate constraint equations should be added to the system:

$$\dot{\varphi}_0^{(H)} = \dot{\tilde{q}}_{j_{HP}}^{(P)}, \tag{39a}$$

$$\dot{\varphi}_{\tilde{n}^{(H)}}^{(H)} = \dot{\tilde{q}}_{j_{HN}}^{(N)} \tag{39b}$$

where $\tilde{q}_{j_{HP}}^{(P)}$ and $\tilde{q}_{j_{HN}}^{(N)}$ are components of vectors $\tilde{\mathbf{q}}^{(P)}$ and $\tilde{\mathbf{q}}^{(N)}$, which relate to rigid finite elements 0 and $\tilde{n}^{(H)}$ of body $(H)$.

### 3.3 Constraint reactions in kinematic pairs

When joint coordinates are applied to description of multibody system kinematics and dynamics, the constraints are introduced only when necessary. In comparison to absolute coordinates, it allows the number of unknown joint reactions and the number of constraint equations to be reduced. Figure 6 presents the spherical joint that connects bodies $(N)$ and $(P)$. Taking into account designations from Fig. 4 and formulae

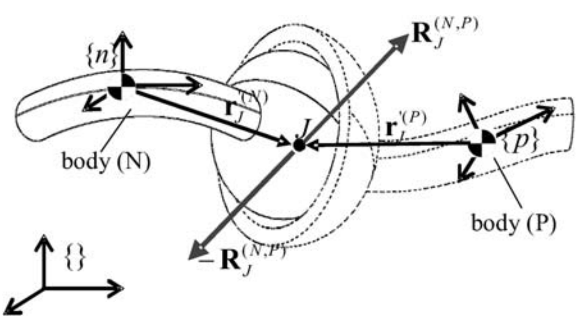


**Fig. 6** Spherical joint connecting bodies $(P)$ and $(N)$

(31a), (32a) and (33a), coordinates of joints $(J)$ in the frame of body $(L)$ are obtained as follows:

$$\mathbf{r}_J^{(L)} = \mathbf{B}^{(L,N)}\mathbf{r}_J^{\prime(N)}, \tag{40a}$$

$$\mathbf{r}_J^{(P)} = \mathbf{B}^{(L,P)}\mathbf{r}_J^{\prime(P)} \tag{40b}$$

where $\mathbf{r}_J^{\prime(N)}$ and $\mathbf{r}_J^{\prime(P)}$ are vectors of coordinates of joint $(J)$ in local frames $\{N\}'$ and $\{P\}'$, respectively.

Assuming that joint reaction

$$\mathbf{R}_J^{(N,P)} = \left[R_{Jx}^{(N,P)} \quad R_{Jy}^{(N,P)} \quad R_{Jz}^{(N,P)} \ 0\right]^T \tag{41}$$

acts with sign + on body $(P)$ and sign − on body $(N)$, the generalized forces arising from joint $(J)$ can be expressed as follows:

$$\mathbf{Q}_{\mathbf{q}^{(L,N)}} = \mathbf{D}_J^{(N)}\mathbf{R}_J^{(N,P)}, \tag{42a}$$

$$\mathbf{Q}_{\mathbf{q}^{(L,P)}} = \mathbf{D}_J^{(P)}\mathbf{R}_J^{(N,P)} \tag{42b}$$

where

$$\mathbf{D}_J^{(N)} = \left(-\mathbf{B}_j^{L,P)}\mathbf{r}_J^{\prime(N)}\right)_{j=1,\dots,\tilde{n}^{(L,N)}},$$

$$\mathbf{D}_J^{(P)} = \left(\mathbf{B}_j^{L,P)}\mathbf{r}_J^{\prime(P)}\right)_{j=1,\dots,\tilde{n}^{(L,P)}}.$$

The coordinates of joint reaction vector $\mathbf{R}_J^{(N,P)}$ are unknown, so spherical joint $(J)$ adds three new unknowns to the system. On the other hand, the first three coordinates of vectors from (40) are the same, so that the constraint equations can be formulated:

$$\theta_j\left[\mathbf{B}^{L,N}\mathbf{r}_J^{\prime(N)} - \mathbf{B}^{(L,P)}\mathbf{r}^{\prime(P)}\right] = 0, \quad \text{for } j = 1, 2, 3 \tag{43}$$

where $\theta_1 = [1\ 0\ 0\ 0]$, $\theta_2 = [0\ 1\ 0\ 0]$, $\theta_3 = [0\ 0\ 1\ 0]$.

Equations (43) can be also written in acceleration form [28].

In a similar way it is possible to obtain the model of prismatic joint (Fig. 7(b)). Both joints from Fig. 7 include five unknowns and involve five constraint equations.

## 4 Application of the method to modeling of a passenger car

On the basis of methods presented in Sects. 2 and 3, the computer programme has been elaborated. Below

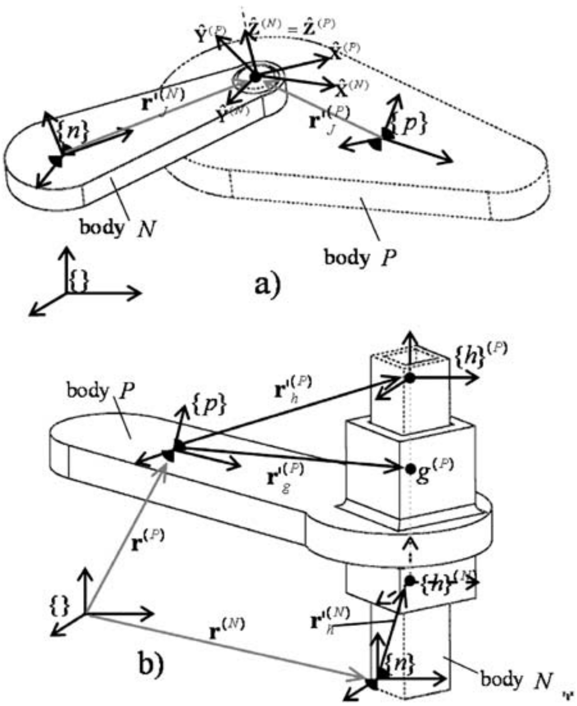


**Fig. 7** Joints connecting bodies $(P)$ and $(N)$ **a** rotational joint, **b** prismatic joint

we present an example of the dynamics of a small passenger car. The model is divided into following subsystems: front McPherson suspension, rear suspension with trailing arms, steering and drive systems, and a tire-road interaction model known as *MagicFormula* [27]. All elements used are listed in Table 1 (abbreviations used: p.b. is name of previous body in chain, NE is the number of elements in the system, $\tilde{N}_b/n_b$ is the number of degrees of freedom in relative motion/total number of generalized coordinates, c-b is the car body, s-r is steering rack, u-s is the upper strut, l-s is lower strut, kn—the knuckle, wh—wheel, t-r is the tie rod, c-a is control arm, s-w is the steering wheel).

As can be seen in Table 1, the vehicle model contains 21 rigid bodies. In Fig. 8, the scheme of the system is presented. The list of joints in the model is presented in Table 2. These elements enable us to take into account closed loops in structural suspension models.

Besides the rigid bodies listed in Table 1, some additional elements with torsional flexibility are taken into account (Table 3).

**Table 1** Elements of vehicle model

| Name | p.b. | $\mathbf{q}^{(\text{body})}$ | $\tilde{N}_b/n_b$ | NE |
|---|---|---|---|---|
| c-b | – | $\mathbf{q}^{(n)} = [x\ y\ z\ \psi\ \theta\ \varphi]^T$ | 6/6 | 1 |
| s-r | c-b | $\mathbf{q}^{(r)} = \begin{bmatrix} \mathbf{q}^{(n)} \\ y^{(r)} \end{bmatrix}$ | 1/7 | 1 |
| u-s | c-b | $\mathbf{q}_k^{(T)} = [\mathbf{q}^{(r)}\ \psi_k^{(T)}\ \theta_k^{(T)}\ \varphi_k^{(T)}]^T$ | 3/9 | 4 |
| l-s | u-s | $\mathbf{q}_k^{(F)} = [\mathbf{q}_k^{(T)}\ z_k^{(F)}\ \psi_k^{(F)}]^T$ | 2/11 | 2 |
| kn | u-s | $\mathbf{q}_k^{(Z)} = [\mathbf{q}_k^{(T)}\ z_k^{(Z)}\ \psi_k^{(Z)}]^T$ | 2/11 | 2 |
| wh | kn | $\mathbf{q}_k^{(W)} = [\mathbf{q}_k^{(Z)}\ \theta_k^{(W)}]^T$ | 1/12 | 4 |
| t-r | s-r | $\mathbf{q}_k^{(D)} = [\mathbf{q}^{(r)}\ \psi_k^{(D)}\ \theta_k^{(W)}\ \varphi_k^{(D)}]^T$ | 3/10 | 2 |
| c-a | c-b | $\mathbf{q}_k^{(H)} = [\mathbf{q}^{(n)}\ \varphi_k^{(H)}]^T$ | 1/7 | 4 |
| s-w | c-b | $\mathbf{q}^{(s)} = [\mathbf{q}^{(n)}\ \psi^{(s)}]^T$ | 1/7 | 1 |

**Table 2** List of joints

| Body $(P)$ | Body $(N)$ | Suspension | Type | Side |
|---|---|---|---|---|
| knuckle | control arm | front | sph. | left/right |
| knuckle | tie rod | front | sph. | left/right |
| lower strut | control arm | rear | sph. | left/right |
| wheel | semi-axle | rear/front | univ. | left/right |

**Table 3** Additional subsystems considered in the model of vehicle

| Name | No. of DoF | Constr. | Description |
|---|---|---|---|
| steering column | $n_{SC}+1$ | 2 | gear ratio<br>dry friction |
| drive shaft | $n_{DS}$ | | torsional flexibility |
| differential | $\varphi_d$ | 2 | differential function<br>dry friction |
| semi-axle | $n_A^{(k)}$ | 2 | wheel and differential connection |

Analysis of Tables 1–3 demonstrates that the number of generalized coordinates and constraints of the whole vehicle is:

$$n_{\text{dof}} = 43 + n_{\text{rfe}} \tag{44a}$$

where $n_{\text{rfe}} = n_{SC} + n_{DS} + n_A^{(l)} + n_A^{(r)}$ is the number of rigid finite elements used in the discretization of

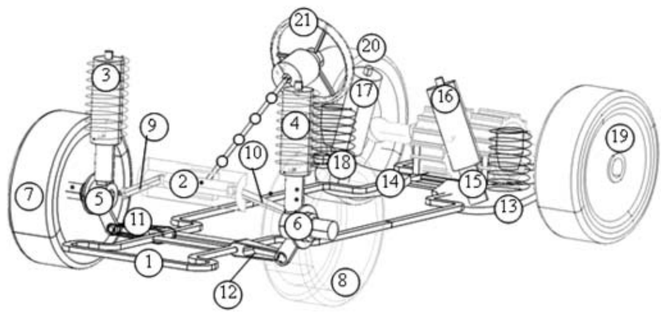


**Fig. 8** General view of the model analyzed

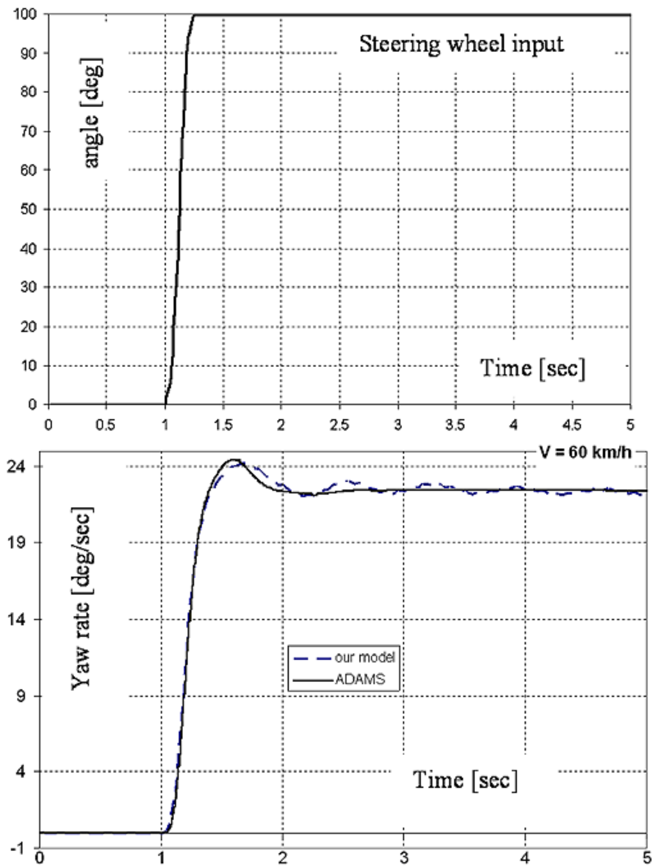


**Fig. 9** **a** Time history of steering input, **b** Comparison of yaw velocity of car

drive and steering subsystems. The number of constraint equation is equal to:

$$n_{\text{constr}} = 26. \tag{44b}$$

In order to perform simulations of vehicle dynamics, a computer programme has been elaborated. It allows us to define the structure of the system (vehicle configuration) and generate the equations of motion, their integration and results post-processing. The complete description of the programme, model and results of experimental verification can be found in [28].

## 5 Calculation results

In this section, the calculation results obtained with our models and programme are compared with results obtained with the ADAMS/Car code [29].

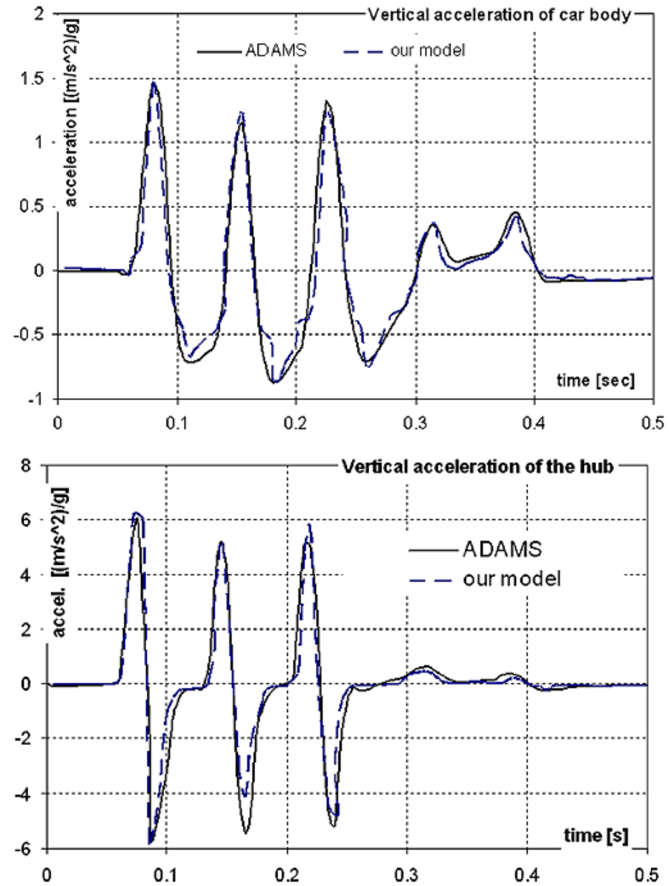


**Fig. 10** Vertical acceleration while passing obstacle: **a** on car body, **b** at the hub

### 5.1 Indirect verification

In the current subsection, we present a comparison of some simulation results obtained from our programme with equivalent ADAMS/Car model (in both cases identical parameters of a small class car have been used). It is important to underline that ADAMS applies the absolute coordinates and $ZXZ$ Euler angles (as default) in the description of multibody dynamics. Three maneuvers are analyzed. First example is concerned with the car motion caused by the steering wheel angle presented in Fig. 9(a). Yaw velocity (with initial longitudinal speed 60 $\frac{\text{km}}{\text{h}}$) of the vehicle is presented in Fig. 9(b)). It can be observed, that the response is almost identical, except for some decaying oscillations produced by our model.

The second simulation concerns motion over three road bumps (with height 0.03 [m]) placed on the road. Wheels on only one side of the vehicle pass over the obstacles. The distance between obstacles is 1 [m]. Figure 10(a) shows vertical acceleration of the car body calculated at the front shock absorber mount, while Fig. 10(b) presents vertical acceleration of the hub. Both are placed on the obstacle-side of the car.

In the last example, low frequency excitation from the road is analyzed. The vehicle runs on a sinusoidal uneven road, with amplitude 1 [cm] and wave length 8 [m]. Time histories presented in Fig. 11 show: (a) the vertical displacements of the center of mass of the car body, and (b) pitch angles.

As in the previous cases, good correspondence of results has been achieved. All results presented here have been obtained with the Runge–Kutta 4th order method of integration of car equations of motion with a constant step size of 0.001 s. The calculation time for a single task varies from 30 s to 5 min. The simulation time in ADAMS/Car was half as long, but with the different methods of integrating the equations of motion (*GSTIFF*).

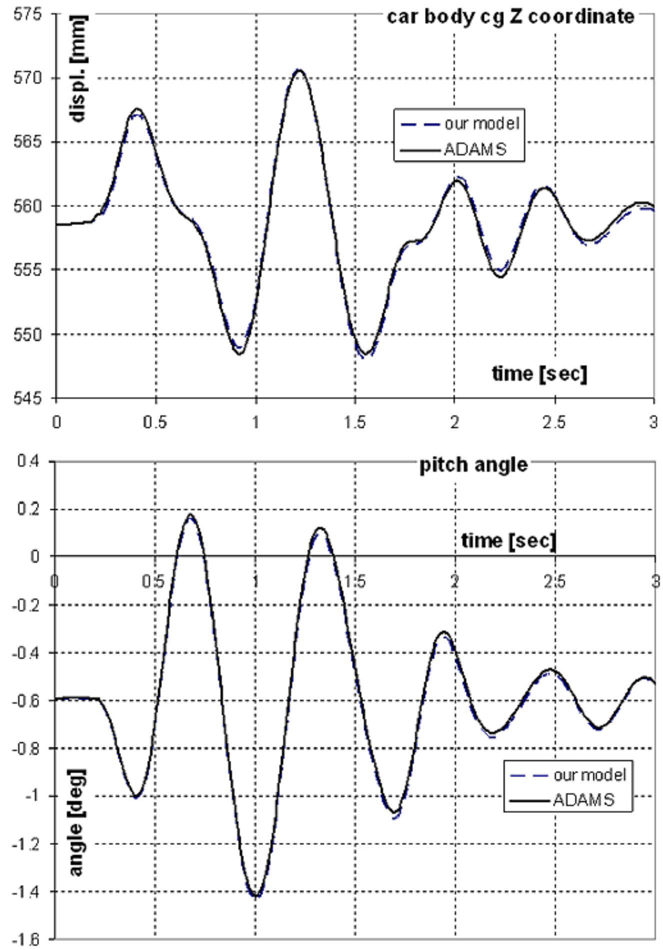


**Fig. 11** Sinusoidal road unevenness **a** car body center of mass, **b** pitch angle

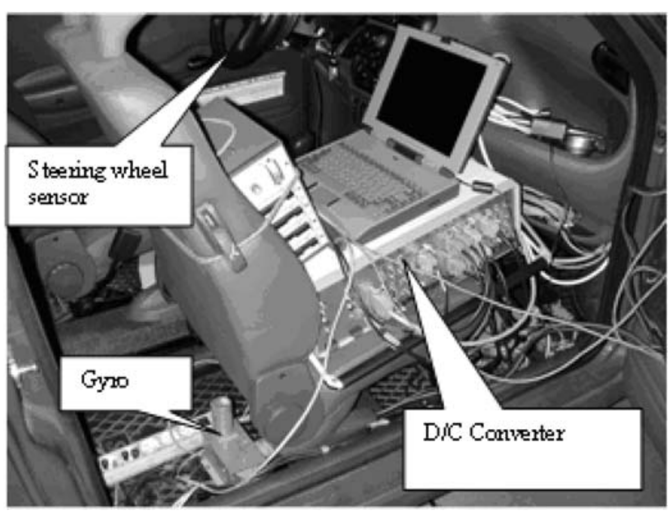


**Fig. 12** Test vehicle with equipment

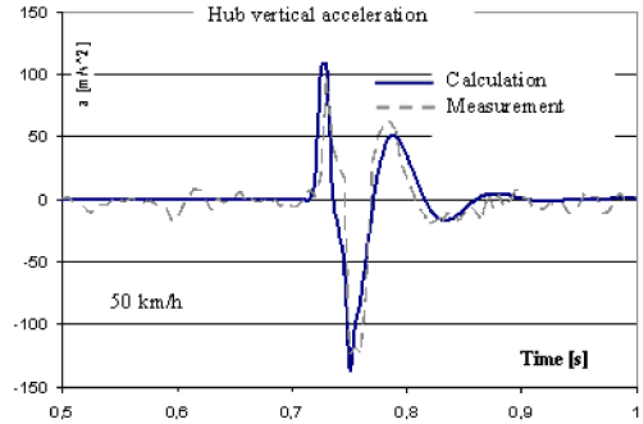


**Fig. 13** Vertical acceleration of the front wheel carrier

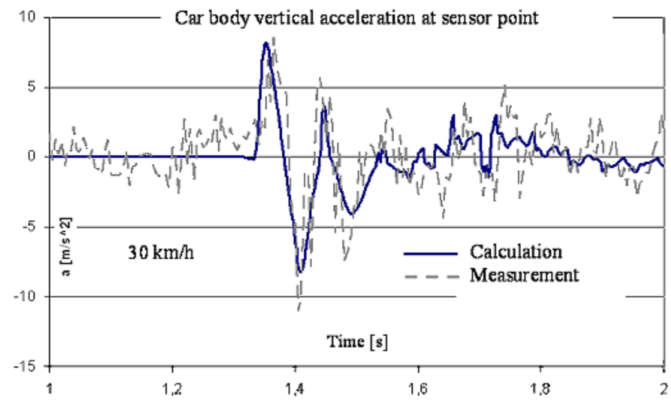


**Fig. 14** Vertical acceleration of the car body

5.2 Direct verification

Below we describe shortly experimental measurements which have been carried out in order to check the correctness of models presented. The vehicle has moved over series of obstacles with sharp edges in such a way that wheels of one side only had been in contact with obstacles on the road. The measurement devices are shown in Fig. 12. The following quantities have been measured:

- vertical acceleration of the car body and front suspension (hub)
- angle and torque of the steering wheel (*Daytona* steering wheel)
- longitudinal and lateral velocities of the car body (Corevit sensor)
- angle of the front wheel

Measurement tests has been performed in different conditions (such as different speed, different motion trajectory, number of obstacles) and some results are presented below. Figures 13 and 14 shows measured and calculated accelerations when the vehicle passed one obstacle. Vertical accelerations of a point of the hub are presented in Fig. 13. In the case presented, the constant speed of the vehicle was about 50 $\frac{\mathrm{km}}{\mathrm{h}}$. Figure 14 shows the acceleration of the car body (the sensor was fixed to the car body close to the column socket of the front left suspension). The speed of the car was equal to 30 $\frac{\mathrm{km}}{\mathrm{h}}$.

The relative errors between calculation results and experimental measurements, estimated by the following formula:

$$\epsilon = \frac{\int_{t_1}^{t_2} |C(t) - M(t)|\, dt}{\int_{t_1}^{t_2} |C(t)|\, dt} 100\% \tag{45}$$

where $C(t)$, $M(t)$ are calculation and measured courses are less than 10%.

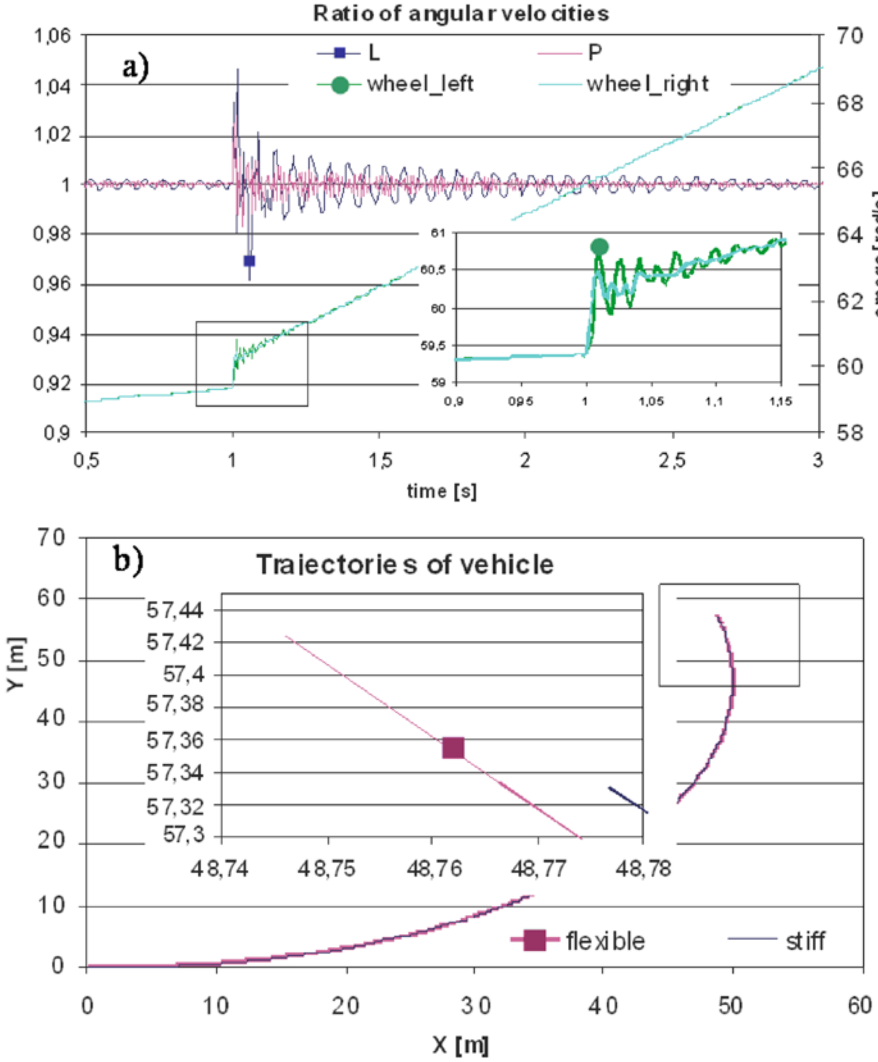


**Fig. 15** Drive system vibrations: **a** rotational speed of driven wheels variation to step torque change, **b** trajectory of the vehicle with rigid and flexible drive system

## 5.3 Influence of flexibility of the drive system on vehicle motion

The elaborated model enables us to analyze dynamics of the drive system and multibody structure of the vehicle. Two models of drive systems have been considered [28]:

- common drive with differential mechanism
- independently driven wheels by electric motors

Figure 15(a) depicts the vibration caused by step-like function of the drive torque generated by electric motors. The test simulation has been performed for the straight motion with initial speed 60 $\frac{\text{km}}{\text{h}}$.

Drive semi-axles have been discretized into 5 rigid finite elements. Different torsional flexibility for the left and right axes has been assumed, which caused the differences in rotational velocity as presented in Fig. 15(a). Vibrations of high frequency are typical for drive systems. It can be seen how vibrations of the axle shaft influence the rotational speed of the driven wheel. Figure 15(b) shows the influence of the flexibility of the drive system on the vehicle trajectory. It seems to be clear that taking into account flexibility of a transmission system has no effect on results concerning global vehicle motion. When general motion of a vehicle is investigated, flexibility of a drive system can be neglected. However, it may be interesting and important in some other tests, for example, starting from the zero point (clutch drop test).

## 6 Final remarks

The paper presents a method of analyzing multibody system dynamics when joint coordinates and homogeneous transformations are applied. The comparison of the results obtained with our model and with the ADAMS/Car package concerns the motion of a small passenger car. A good correspondence of calculation results has been achieved. Differences are caused not only by the different methods applied, but mainly by different methods of integrating the equations of motion of a car. In our opinion, the comparison of calculation and experimental results confirms correctness of the mathematical models and programmes developed despite some differences which are due to simplifications or random input. Presented models and methods have general character, they can be used for numerical analysis of multibody systems in different applications. Few simplified versions of the model have been used in optimization and control tasks. Papers [30, 31] present the calculation results obtained for different methods of integration. In comparison with [30], the analysis presented in [31] is concerned with additional complex maneuvers. The methods in those papers include methods with an adaptive time step and methods for stiff systems of differential ordinary equations. The results presented in [31] show how the model complexity and integration methods affect calculation time.

The methods and programme presented in the paper have been also successfully applied to dynamic analysis of articulated vehicles [20, 21]. The main disadvantage of the method presented results from (28). When joint coordinates are used, the body attached changes the equations of motion of the preceding chain of bodies. On the other hand, the main advantage is that the number of generalized coordinates and in consequence, the number of equations of motion that have to be solved is minimal. In cases when a reaction in joints has to be calculated (e.g. when dry friction in joints is considered), the numerically effective Newton–Euler algorithm can be used [24, 32].

The method presented in the paper allows us to describe the motion of vehicles using the methods developed for kinematic and dynamic analysis of manipulators. In the approach presented, the joint coordinates and homogeneous transformations can be used for description of a system with rigid and flexible links. The method is simple and uniform. As it is shown in [26], large deformation of flexible elements can also be taken into account. However, the authors' experience shows that until now the numerical efficiency of the method is not comparable with methods applied in commercial packages when large structures are simulated. We hope that the presented method can be successfully applied when simplified models for particular applications are formulated.

**Acknowledgements** This paper was written as part of Project 4T07A04928 financed by the Polish Committee for Scientific Research.

## References

1. Wittenburg, J.: Dynamics of Systems of Rigid Bodies. Teubner, Stuttgart (1977)
2. Shabana, A.A.: Dynamics of Multibody Systems. Willey, New York (1989)
3. de Jalon, J.G., Bayo, E.: Kinematic and Dynamic Simulation of Multibody Systems. The Real-Time Challenge. Springer, New York (1994)
4. Schiehlen, W.: Multibody system dynamics: roots and perspectives. Multibody Syst. Dyn. **1**, 149–188 (1997)
5. Gear, C.W.: Differential-algebraic equation index transformations. SIAM J. Sci. Stat. Comput. **9**, 39–47 (1988)
6. Petzold, L.R.: An efficient numerical method for solving stiff and nonstiff systems of ordinary differential equations. SIAM J. Numer. Anal. **18**, 455–479 (1981)
7. Baumgarte, J.: Stabilisation of constraints and integrals of motion in dynamical systems. Comput. Methods Appl. Mech. Eng. **1**, 1–16 (1972)
8. Arnold, M.: Simulation algorithms in vehicle system dynamics. Reports on Numerical Mathematics, Martin-Luther University Halle-Wittenberg, 04–27 (2004)
9. Blundell, M.V.: The modeling and simulation of vehicle handling. Part 1: analysis method, Part 2: vehicle modeling. Proc. Inst. Mech. Eng. **213**(Part K), 103–134 (1999)
10. Hegazy, S., Rahnejat, H., Hussain, K.: Multi-body dynamics in full-vehicle handling analysis under transient maneuver. Veh. Syst. Dyn. **34**, 1–24 (2000)
11. Iwnicki, S.: Simulation of wheel-rail contact forces. Fatigue Fract. Eng. Mater. Struct. **26**, 887–900 (2003)
12. Mousseau, C.W., Laursen, T.A., Lidberg, R.L., Taylor, R.L.: Vehicle dynamics simulations with coupled multibody and finite element models. Finite Elem. Anal. Des. **31**, 295–315 (1999)
13. Ambrosio, J.A., Goncalves, J.P.: Complex flexible multibody systems with application to vehicle dynamics. Multibody Syst. Dyn. **6**(2), 213–227 (2001)
14. Savaresi, S.M., Bittanti, S., Montiglio, M.: Identification of semi-physical and black-box non-linear models: the case of MR-dampers for vehicles control. Automatica **41**, 113–127 (2005)

15. Ieluzzi, M., Turco, P., Montiglio, M.: Development of a heavy truck semi-active suspension control. Control Eng. Pract. **14**, 305–312 (2006)
16. Valasek, M., Kortum, W., Sika, Z., Magdolen, L., Vaculin, O.: Development of semi-active road-friendly truck suspensions. Control Eng. Pract. **6**, 735–744 (1998)
17. Vaculin, O., Valasek, M., Krüger, W.R.: Overview of coupling of multibody and control engineering tools. Veh. Syst. Dyn. **41**, 415–429 (2004)
18. Attia, A.A.: Computational dynamics of three-dimensional closed-chains of rigid bodies. Appl. Math. Comput. **172**, 286–304 (2006)
19. Kim, S.: A subsystem synthesis method for efficient vehicle multibody dynamics. Multibody Syst. Dyn. **7**(2), 189–207 (2002)
20. Grzegożek, W., Adamiec-Wójcik, I., Wojciech, S.: Computer Modelling of Vehicle Dynamics. Press of TU Cracow, Cracow (2003) (in Polish)
21. Adamiec-Wójcik, I.: Modelling dynamics of multibody systems using homogeneous transformations. Scientific Papers of University of Bielsko-Biała, 3 (2003)
22. Denavit, J., Hartenberg, R.S.: A kinematic notation for lower-pair mechanisms based on matrices. J. Appl. Mech. **2**, 215–222 (1955)
23. Paul, R.P.: Robot Manipulators: Mathematics, Programming, and Control. MIT Press, Cambridge (1981)
24. Craig, J.J.: Introduction to Robotics. Addison–Wesley, Massachusetts (1988)
25. Blajer, W.: Methods of Multibody System Dynamics. Press of TU Radom, Radom (1998)
26. Wittbrodt, E., Adamiec Wójcik, I., Wojciech, S.: Dynamics of Flexible Multibody Systems. The Rigid Finite Element Method. Springer, New York (2006)
27. Pacejka, H.B.: Tyre and Vehicle Dynamics. SAE Inc, Warrendale (2002)
28. Szczotka, M.: Modelling of vehicle dynamics taking into account various drive systems. PhD dissertation, University of Bielsko-Biała (2004)
29. MSC.ADAMS/Car Documentation, MSC. Software Corporation (2005)
30. Szczotka, M., Tengler, S., Wojciech, S.: Application of joint co-ordinates and homogeneous transformation to modeling car dynamics. In: Proceedings of 8th Conference on Dynamical Systems, Theory and Applications, pp. 801–808. Lodz (2005)
31. Szczotka, M., Tengler, S., Wojciech, S.: Numerical effectiveness of models and methods of integration of the equations of motion of a car. Differ. Equ. Nonlinear Mech., doi: 10.1155/2007/49157 (2007)
32. Wojciech, S.: Dynamic analysis of manipulators with considerations of dry friction. Comput. Struct. **6**, 1045–1050 (1995)